POTENTIAL INJURY CRITERIA FOR COLLISIONS WITH HEAVY GOODS VEHICLES

Jason Forman[1], Martin Östling[2], Krystoffer Mroz[2], Nils Lubbe[2]
1 University of Virginia Center for Applied Biomechanics
2 Autoliv Research Sweden

Paper Number 23-0334

ABSTRACT

Background:

Collisions with heavy goods vehicles (HGVs, large trucks) comprise approximately 21% of fatalities in two-vehicle collisions in the United States, and 14-15% of car occupant fatalities in Europe. While the immediate need in these collisions lies in compatibility and the structural integrity of the smaller vehicle, once these are addressed it will be up to the restraint system to manage protection of the occupants at collision severities that are greater than are commonly evaluated now. For restraint evaluation in high-severity collisions where survivability is the focus, different injury criteria targets may be warranted, focused on balancing injury risk across the body regions to fully utilize the load-bearing capability across the body. In this study we seek to identify potential injury criteria target values (and knowledge gaps) for predicting injury risk across the body in evaluations of high-severity collisions.

Methods and Data Sources:

This study consisted of a literature review, combined with a field data analysis to contextualize the types and distributions of injuries that occur among collisions of various severity. Data from NASS-CDS (years 2010-2015) and CISS (years 2017-2019) were examined to observe the relative distribution of injury severities by injury type, focusing on belted occupants in frontal collisions. Contemporary injury risk functions were then reviewed (using exemplar high-severity collision simulations) to observe the relative injury risks predicted across the body in collision severities representative of car-to-HGV collisions. Injury risks were further evaluated in high-severity collision simulations with an improved restraint system designed to manage occupant energy in such scenarios, demonstrating that injury risk can be reduced by adapting the restraint system to the severity of the crash.

Results and Discussion:

Across collision severities, injury risks were relatively balanced among the body regions. Most AIS2+ and AIS3+ injury cases occurred in relatively low-severity collisions, due to the very high exposure to low-severity collisions. AIS4+ injury cases occurred with similar total counts in low-severity and high-severity collisions, affected by the balance of exposure and per-crash risk. In high-severity collisions, the most common injury types were to the ankle, tibia & fibula, brain, thorax, and lumbar spine, all occurring with similar frequency. In simulations with the THOR-50M finite element model in high-severity impact scenarios, the injury risk predicted across the body regions exhibits similar balance to that observed in the field data, except for the risks predicted in the chest and the hip. Upon examination of the risks observed in the field data, as well as those observed in high-severity impact simulations with different restraint systems, injury assessment reference values were developed targeting a risk of 40%, representing a target that is feasible to achieve and which has a high likelihood of providing a tangible benefit to the field.

Conclusions:

Injuries occur as a result of both exposure and per-incident risk. Injury reduction likely requires safety systems that can adapt to the crash severity, providing more compliant restraint in low-severity collisions (where the exposure is very high), and stiffer restraint designed to eliminate strike-through in higher severity collisions (where the per-crash risk is high). Such adaptive-restraint design requires injury risk targets designed for the specific collision severities targeted for evaluation – including more conservative targets for low-severity evaluations, and higher practical targets for high-severity evaluations (focusing on survivability). This study has identified potential means for defining injury criteria values specifically for evaluations in high-severity collision scenarios, targeting a balance among the body regions informed by recent field data.

INTRODUCTION

Car-to-heavy goods vehicle (C2HGV) collisions comprise approximately 14-15% of the car occupant fatalities in Europe [1-3], and 21% of the car occupant fatalities in the U.S. in two-vehicle crashes [4]. Until now, most efforts to address crashworthiness considerations for C2HGV collisions have focused on geometric compatibility and the structural integrity of the passenger vehicle. Prior to the push for improved compatibility, many of the C2HGV collisions in the U.S. were prone to underride of the passenger vehicle, resulting in loading of the occupant compartment with limited engagement of the elements designed for structural crashworthiness [5-9]. Even once geometric compatibility concerns are addressed, however, there remain challenges in mass compatibility and the structural integrity of the passenger vehicle. Heavy goods vehicles (e.g., loaded tractor trailers) tend to be roughly 10 times the mass of typical passenger vehicles. As a result of the difference in momentum of the collision partner, collisions with heavy goods vehicles can result in very high ΔVs in smaller vehicle, meeting or exceeding the smaller vehicle's initial over-the-ground speed (often at highway speeds, and often with limited overlap [10]). Collisions of such severity can exceed those typically assessed in standardized regulatory or consumer information crash test modes, and can challenge the structural integrity of the smaller vehicle. The first countermeasure for such collisions will lie in improving geometric compatibility and the passenger vehicle structure to preserve occupant compartment integrity in such collisions. Once occupant compartment integrity is ensured, however, the next challenge will lie in providing adequate occupant restraint in the face of very high severity ΔV pulses [10-11]. This may be aided by energy-absorbing countermeasures integrated into the heavy-goods vehicle, designed to stretch out the collision pulse and decrease the acceleration magnitude imparted to the smaller vehicle [12]. The final step in the protection chain will rely on restraint systems tuned to manage the occupant's energy and momentum when faced with a large change in velocity.

This study contemplates future needs for addressing occupant restraint in high severity collisions associated with either C2HGV crashes or high speed C2C crashes, after compatibility and structural integrity are addressed. In particular, future efforts to evaluate restraint performance in high severity collisions will require targets for Injury Assessment Reference Values for injury criteria tailored to feasible target values that represent an improvement relative to the current state of the field, while still presenting a target that is feasible to achieve with conceivable restraint systems. To develop such safety systems, we need target injury criteria that capture measures pertinent to injuries that occur in the field, while also presenting targets that may feasibly addressed through refinement of restraint-based occupant protection systems.

The goal of this study was to identify potential field-relevant injury criteria (and associated target thresholds) that may aid in reducing injury risk in high-severity collisions.. To identify the injury types to target, we examine field data for frontal impact collisions with belted occupants across multiple collision severity ranges. These data also will serve to identify relative rates of injury among the various body regions, providing insight into whether the risk for certain body regions is higher than others. Similarly, by comparing across multiple collision severity ranges we can observe the progression of risk, elucidating whether certain injury types become disproportionately more common in higher severity collisions compared to the relative distribution of injuries in low-to-moderate severity collisions. Such an analysis also provides context for the relative frequency of injury across ΔV ranges, including the combined effects of exposure and per-crash injury risk. Finally, results from an exemplar set of simulations with the THOR-M50 model were examined to observe injury risks calculated from injury criteria that have been proposed for that anthropomorphic test device (ATD) compared to the risks indicated by the field data. By combining the field data observations with the injury risks calculated from the exemplar simulations, we discuss potential options for injury criteria and target threshold values that capture the balance of injury risks observed across the various body regions in the field, while providing targets that would represent improvements to the current state of risk in the field.

METHODS & RESULTS

The National Automotive Sampling System Crashworthiness Data System (NASS-CDSS) and the U.S. Crash Investigation Sampling System (CISS) were both queried to observe the relative distributions of injuries for belted occupants of passenger vehicles (sedan, MPV, SUV, light truck, etc.) in frontal collisions across three categories of collision severity: 0-34 km/h ΔV, 35-59 km/h ΔV, and 60+ km/h ΔV. Data were queried from NASS-CDS collection years 2010-2015 and CISS collection years 2017-2019, each with vehicles ≤ 10 years old at the time of the collision. Frontal impact collisions were examined, defined based on a PDOF from 300º-60º with a General Area of Damage (GAD) code of F (Front) or L/R if the horizontal location was coded as Front. Belted occupants age 13+ were examined. Rollovers, fires, and ejections were excluded. Injuries were examined by body region and by AIS level, using the most recent version of AIS available for each case collection year. The body region categories are for the most part self explanatory. To clarify for those injury types were there may be some ambiguity – hip injuries included injuries to the proximal femur (femoral neck and above) as well as the acetabulum; femur injuries included fractures to the middle and distal femur not counted in the hip injury category (to avoid double-counting); pelvis injuries included all pelvis injuries except for acetabulum injuries; and ankle injuries included injuries to the distal tibia and fibula (which were excluded from the tibia/fibula category to avoid double-counting), injuries to the talus, injuries to the calcaneus, and ankle ligament injuries of the target severity category.

The distributions of injury types for the three ΔV categories are shown in Figure 1 (unweighted results) and Figure 2 (weighted results) below. Note that in the weighted analysis one case from the middle ΔV category (35-59 km/h) was removed because it had a very high weight (over 4,000) and had fractures in each of the spine regions, which caused spine fractures to appear to comprise a larger portion of the injury distribution in that ΔV range than they likely do. All other observations were relatively consistent between the unweighted and weighted distributions.

In the lowest ΔV range (0-34 km/h), the vast majority (over 85%, weighted) of injury cases only had a maximum AIS severity (MAIS) of 2. Approximately 10% of injury cases (weighted) were MAIS 3. Less than 3% of injury cases in that category were MAIS 4+. For the MAIS 2 cases in that ΔV range, brain injuries were the most common injury type among the injury types studied. This was followed by thoracic organ injury, lumbar spine injury, tibia/fibula and ankle injury, and abdomen injury. The most common MAIS 3 injuries were rib fractures. For the mid ΔV range (35-59 km/h), the most common AIS2 injuries were to the tibia/fibula and ankle, lumbar spine, brain, and thoracic organs. The most common AIS 3 injuries were rib fractures and femur fractures. For the higher ΔV range (60+ km/h), the most common AIS2 injuries were similar to those of the 35-59 km/h range (i.e., tibia/fibula and ankle, lumbar spine, brain, and thoracic organs). The most common AIS 3 injuries were thoracic organ injuries, rib fractures, and femur fractures. The most common AIS4+ injuries were brain and abdomen injuries. Considering relative frequencies - across all ΔV ranges - femur fractures occurred with greater frequency than hip or pelvis injuries. In the 60+ km/h ΔV range, there is a relatively even balance in injury frequency between rib fractures, femur fractures, and brain injury.

Figures 1 and 2 also show the total number of collision exposures in the dataset for each ΔV range. When survey weights are applied (Figure 2), approximately 3.7 million people were exposed to collisions in the 0-34 km/h ΔV range , 274 thousand people were exposed to collisions in the 35-59 km/h ΔV range, and 23 thousand people were exposed to collisions in the 60+ km/h ΔV range. Table 1 shows the per-crash injury risk for each AIS level for each ΔV range. For crashes in the 0-34 km/h ΔV range, there is a 3.7% chance that any individual crash will result in AIS2+ injury. For crashes in the 60+ km/h ΔV range, there is a 46% chance that any individual crash will result in AIS2+ injury. The risks decrease for each elevated AIS level. The per-crash risk for AIS3+ injury is 0.46% for the 0-34 km/h ΔV range, and 27% for the 60+ km/h ΔV range. The risk is decreased to 0.09% and 13.7%, respectively, for AIS4+ injury.

Table 1: Injury risk calculated from the field data (count of injury cases divided by count of exposures) for each ΔV range, by AIS severity level (weighted)

Per-Crash Risk (weighted)			
	0-34 km/h	35-59 km/h	60+ km/h
AIS2+	3.72%	16.0%	46.3%
AIS3+	0.46%	5.07%	26.9%
AIS4+	0.09%	0.41%	13.7%

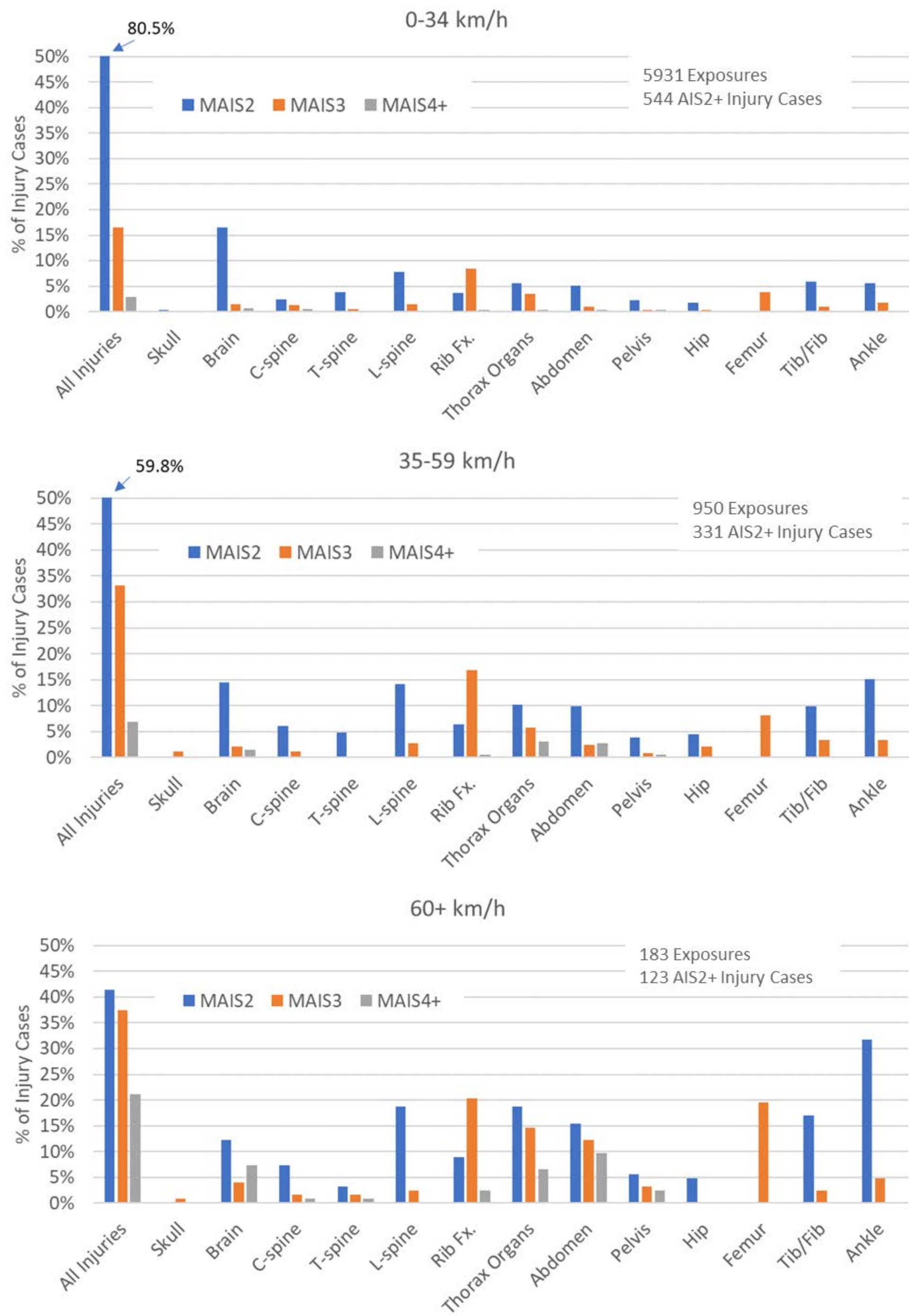

Figure 1: Unweighted distribution of injured body regions by ΔV range and AIS severity level (belted occupants in frontal collisions, in vehicles less than 10 years old at the time of the collision; NASS-CDS 2010-2015 and CISS 2017-2019). [Note: The injury types shown here were selected based on injury types that may conceivably be predicted using ATD-based measures. There are some other injury types that occurred with considerable frequency but are not shown here (e.g., sternum fractures). Those contribute to the "All Injuries" count, but are not shown in the individual body regions.]

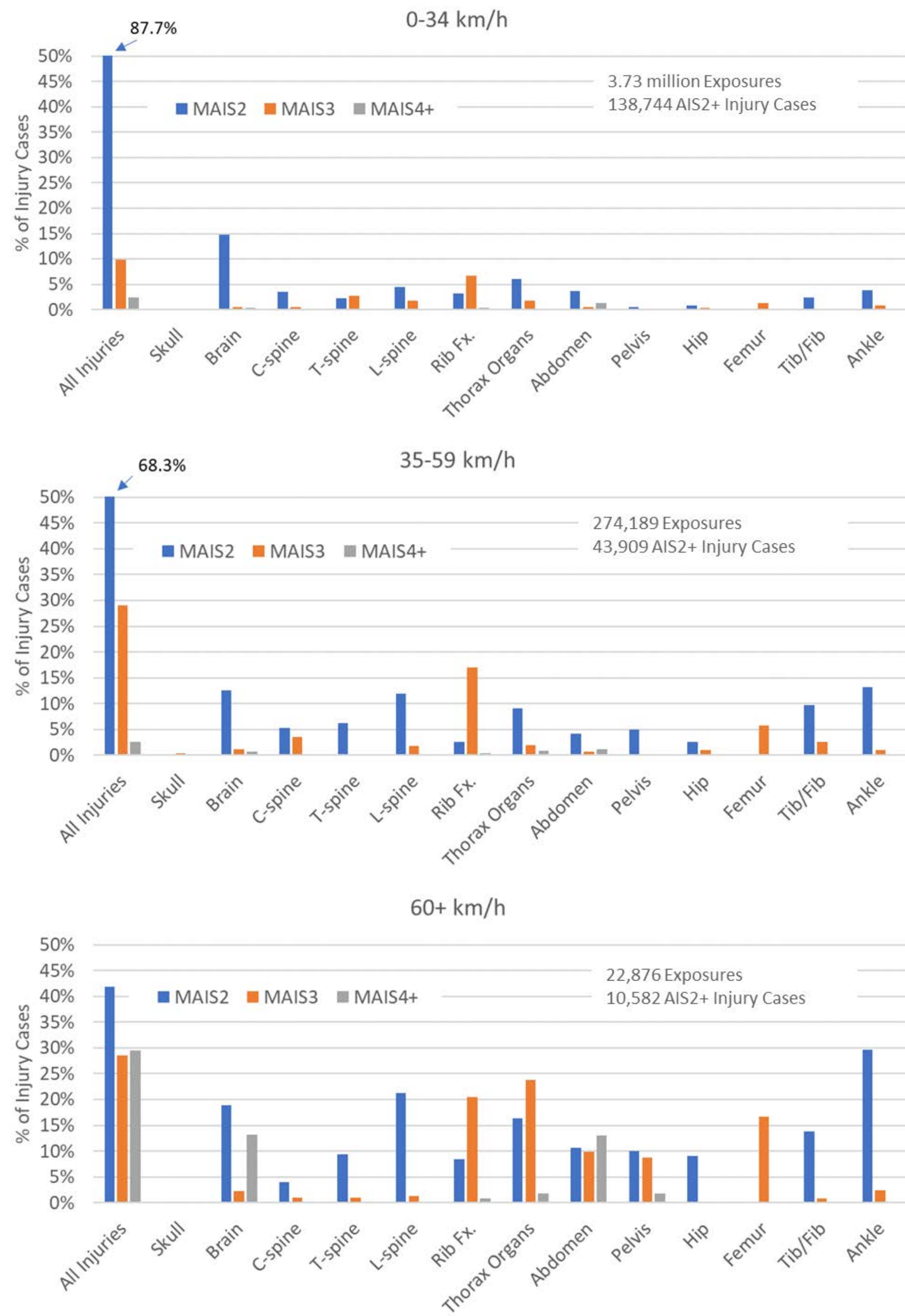

Figure 2: <u>Weighted</u> distribution of injured body regions by ΔV range and AIS severity level (belted occupants in frontal collisions, in vehicles less than 10 years old at the time of the collision; NASS-CDS 2010-2015 and CISS 2017-2019). [Note: The injury types shown here were selected based on injury types that may conceivably be predicted using ATD-based measures. There are some other injury types that occurred with considerable frequency but are not shown here (e.g., sternum fractures). Those contribute to the "All Injuries" count, but are not shown in the individual body regions.]

Table 2 shows the distribution of injuries by ΔV, capturing the combined effects of exposure and per-crash risk. Applying the survey weights, 72% of cases of AIS2+ injury occur with ΔV's in the 0-34 km/h range, presumably due to the very high exposure of crashes in that range. The proportion of injury cases in the 60+ km/h ΔV range increases to 17% and 41% for AIS3+ and AIS4+ injury, respectively. Unweighted distributions are also presented for context, naturally showing a decrease in the proportion comprised by low-severity crashes (due to the intentional under-sampling of low-severity crashes in NASS-CDS and CISS, which is then corrected for by applying the survey weights).

Table 2: Distribution of injury cases by ΔV range.

Weighted % of injury cases that each ΔV category comprises				
	0-34 km/h	35-59 km/h	60+ km/h	N†
AIS2+	72%	23%	5%	197,609
AIS3+	46%	37%	17%	37,161
AIS4+	44%	15%	41%	7,600
N*	138,755	48,281	10,582	--
Age**	48.9	52.3	41.2	
Unweighted % of injury cases that each ΔV category comprises				
	0-34 km/h	35-59 km/h	60+ km/h	N†
AIS2+	55%	33%	12%	998
AIS3+	34%	43%	23%	311
AIS4+	25%	35%	40%	65
N*	544	331	123	--
Age**	49.6	45.3	39.8	

* Number of AIS2+ injury cases within each ΔV range.
** Average age (in years) of AIS2+ injured occupants within each ΔV range.
† Total number of injury cases of each AIS level, summing across the ΔV ranges.

To compare to the injury frequency distributions noted above, injury risks were calculated for a series of exemplar simulations described in a parallel study by Östling et al. [11]. That study simulated collisions representing car-to-heavy goods vehicle crashes (C2HGV) with two different pulses (a long-duration pulse of approximately 40 g plateau, and a short-duration pulse of approximately 85 g plateau [10-11]) with a contemporary restraint system, and with a restraint system improved to reduce injury criteria values in such a collision (details described in [11]). That study also simulated a 56 km/h full frontal rigid barrier crash (FFRB) for comparison. Those simulations were performed with the THOR-50M v1.9 Euro NCAP occupant model distributed by Humanetics Inc., and injury risks were calculated using the injury risk functions (IRFs) described by Craig et al. [13] (Table 3). For the chest, injury risk was calculated using the IRFs developed for prediction of 3+ rib fractures and 6+ rib fractures described by Craig et al. [13] (2020). For the hip injury risk predicted from the force measured by the acetabulum load cells, the risk was calculated for both a 15º hip flexion angle and a 0º hip flexion angle using the functions described by Craig et al. [13]. For all other body regions, injury risk was calculated using the final IRFs ultimately recommended by Craig et al. [13].

As can be seen in Table 3, from these simulations the THOR measurements and the IRFs of Craig et al. [13] resulted in relatively balanced injury risks predicted for the brain, femur, abdomen, and tibia. The chest injury risk predicted with the IRF designed for 3+ rib fractures tended to result in a predicted risk that was disproportionately higher than the other body regions. The chest injury risk predicted with the IRF designed for 6+ rib fractures tended to result in a predicted risk that was more balanced with the other body regions.

Table 3: ATD measures and associated risk predictions from exemplar simulations with the THOR-50M*

Crash pulse		56 km/h FFRB		Car-to-HGV High Acc. Pulse – Contemporary Restraint System		Car-to-HGV High Acc. Pulse – Improved Restraint System	
	Unit	**Value**	**Risk**	**Value**	**Risk**	**Value**	**Value**
HIC15 (AIS3+)		365	2%	2162	62%	1382	38%
BrIC (AIS3+)		0.55	1%	1.15	74%	0.85	33%
Nij (AIS3+)		0.32	1%	1.42	84%	0.98	33%
Chest deflection (3+ fracture 40 years)	mm	40.4	29%	56.8	61%	56.4	60%
Chest deflection (6+ fractures 40 years)	mm	40.4	17%	56.8	41%	56.4	40%
Acetabulum resultant force (AIS2+), 15°	N	3851	71%	20813	100%	5667	99%
Acetabulum resultant force (AIS2+), 0°	N	3851	37%	20813	100%	5667	91%
Femur compression (AIS2+)	N	2683	0%	34697	100%	9742	39%
Upper Tibia axial force (AIS2+)	kN	1.6	1%	11.0	96%	3.3	5%
Lower Tibia axial force (AIS2+)	kN	1.8	5%	6.9	38%	3.4	10%
Tibia bending moment (AIS2+)	Nm	104	2%	1145	100%	234	22%
Revised Tibia index (AIS2+)		0.53	5%	5.68	100%	1.23	49%

* Risks calculated using the injury risk functions described by Craig et al. [13], from the simulation results described by [11].

Each of the predicted injury risks decreased in the C2HGV simulations with the improved restraint system (decreasing from roughly 60-100% risk with the contemporary restraint system to 40% or less across most body regions with the improved system). The one apparent outlier was the injury risk predicted using the force measured in the acetabulum load cell, which was substantially higher than the risk predicted for the other body regions (including the femur) for both the C2HGV simulations with the improved restraint system, and the reference simulations representing a lower-severity 56 km/h FFRB condition.

DISCUSSION

Balance of Risk and Implications in Injury Prediction

Optimal restraint design relies on a balance of injury risk throughout the body. To decelerate a person during a collision, we need to apply force to the body. Wherever we apply force to the body, there is a risk that force may result in injury. The key is to apply retraining force to the body in a distributed fashion designed to utilize the load-bearing capacity of every body region, while mitigating the risk that any particular body region will be over-loaded and injured. In an ideal case, the restraint system will be designed to load every body region up to the very threshold of its load bearing capability, but not over. To maximize the potential efficiency of a restraint system in this manner, we need to understand the balance of injury tolerance and injury risk throughout the body, and replicate that balance in our injury prediction tools.

The results above suggest that in most collisions, injury frequency is relatively balanced between brain injury, rib fracture injury, tibia/fibula fractures, and femur fractures. Ankle fractures also occur with considerable frequency in collisions above 35 km/h, though those injuries are challenging to monitor by dummy measures in standardized crash tests [14]. Aside from ankle fractures, the balance of injury frequency across body regions is relatively consistent with the balance of risks observed in the injury predictions of Table 3. The chest injury risks predicted with the 3+ rib fracture function tended to predict risks somewhat higher than the other body regions, contrary to the relative rates observed in the field data. This was improved with the chest injury risks predicted with the 6+ rib fracture function, which resulted in risks more consistent with those observed in the other body regions [11].

The balance of injury risks predicted by the injury criteria of Table 3 also carry through across the other conditions studied, with each body region exhibiting a decrease in risk with the improved restraint system applied to the C2HGV collision, and in the lower severity 56 km/h reference simulations. In each of these cases (the improved restraint system, and the 56 km/h reference case) the injury risk decreases by similar amounts for the head, neck, chest, and femur injury measures. For the C2HGV simulations with the improved restraints, the risks across most of those body regions decrease from approximately 60-100% risk with the contemporary restraints, to approximately 40% risk with the improved restraints. The risk for chest injury remained elevated using the 3+ fracture definition, but as noted above was more consistently balanced with the other body regions using the 6+ fracture definition. For most body regions the risks are further reduced below approximately 20-30% in the reference 56 km/h reference simulations.

The one notable exception in terms of both balance and reduction in risk lies in the acetabulum injury measures. Using the acetabulum force IRF of Craig et al. [13], the predicted risk of hip & acetabulum injury is consistently higher than the other body regions in a manner that is not consistent with the relative frequency of injuries that occur in the field. For example, the predicted risk of hip & acetabulum injury from the THOR simulations is consistently higher than the risk predicted for femur injury (even with the improved restraints and lower collision ΔV). This is contrary to the field data, which show that femur fractures occur at a much higher frequency than hip & acetabulum injuries (Figure 1 and 2). While the risk of most injury types is substantially reduced with the improved restraints in the C2HGV condition, and in the reference 56 km/h condition, the risk predicted from the acetabulum load cells remain high even for the improved-restraint and lower speed conditions. These observations are contrary to the field data, which suggest that the injury risks for the various body regions should be relatively balanced, and the risk predicted for the hips should be less than the risk predicted for the femurs.

Injury Assessment Reference Values Based on Target Risk Thresholds

In the development of restraint systems to improve protection in high severity crashes, we need injury criteria targets to design towards. These targets need to strike a balance between being feasible to achieve, while still challenging enough to drive improvement. There are many different ways that such target thresholds can be identified, and the thresholds can be changed over time to continue to drive improvement as safety systems are refined. For example, target injury criteria may be identified by examining current risks exhibited in the field data, combined with risks predicted with contemporary restraint systems. As noted in Table 1, for the 60+ km/h ΔV range the risk of AIS2+ injury is approximately 46%. As noted in Table 3, the risk predicted in the C2HGV simulations with a contemporary restraint system ranged from approximately 60-100%. Aside from the acetabulum, these risks decreased with the improved restraint system, falling under 40% risk for most body regions (once the chest injury risk is predicted with the 6+ rib fracture function). Considering this, a target predicted risk of 40% may represent an achievable goal – if the risks predicted from the injury criteria are indicative of risk in the field, a goal of 40% would also present a target that would improve risk compared to the current state of the field. Note also that the improved restraint system described here would not immediately achieve the goal of <40% predicted risk – further refinement would be needed to drop the risk predicted for some body regions below that target. Once a target risk threshold is identified, this may be translated into target injury criteria values using the associated injury risk functions. An example of target injury criteria values based on a threshold of 40% risk is shown in Table 4. [Note that these targets would apply to a goal of <40% risk in any individual body region. Calculating aggregated risk across the whole body would require a combined probability approach similar to that used by U.S. NCAP, however these individual targets may serve as a reasonable first step for initial improvements.]

Table 4: Example THOR-50M Injury Assessment Reference Values for high severity crash evaluation, targeting a 40% risk threshold.*

Criteria	Unit	Risk	Value
HIC15 (AIS3+)		40%	1430
BrIC (AIS3+)		40%	0.89
Nij (AIS3+)	mm	40%	1.04
Chest deflection (3+ fracture 40 years)	mm	40%	46.5
Chest deflection (6+ fracture 40 years)	mm	40%	56.5
Acetabulum resultant force (AIS2+), 15° Femur flexion	N	40%	3180
Acetabulum resultant force (AIS2+), 0° Femur flexion	N	40%	3910
Femur compression force (AIS2+)	N	40%	9800
Upper Tibia axial force (AIS2+)	kN	40%	6.5
Lower Tibia axial force (AIS2+)	kN	40%	7.15
Tibia bending moment (AIS2+)	Nm	40%	290
Revised Tibia index (AIS2+)		40%	1.13

* Note: These simply represent the values that result from direct calculation via the IRFs of Craig et al. (2020) at the shown risk level. Additional investigation is needed to determine if these are actually achievable with the THOR-50M.

Low-to-Moderate Speed Collisions with High Exposure

While the highest individual per-crash risks were observed in the 60+ ΔV range, most injury cases actually occurred in the 0-34 km/h ΔV range due to the very high collision exposure in that range. As shown in Figure 2, there are an order of magnitude more collision exposures in the 0-34 km/h ΔV range compared to the 35-59 km/h ΔV range. There is a further order of magnitude decrease moving to the 60+ km/h ΔV range. As a result, even though the per-crash risk in the 0-34 km/h range is quite low, the very high exposure causes there to be more injury cases in that range compared to the other ranges. As a result, it may be pertinent to consider continuing improvements to drive down risk in that range even further, in addition to refinements implemented targeting cases with high per-crash risk. This may require safety systems with increased adaptation and sensing capabilities, including refined classification of the collision severity (potentially with classification of the closing speed between the two vehicles, and the size/class of the collision partner).

Risk threshold targets for the 0-34 km/h ΔV range may be developed using a process similar to that described above, for example targeting a very low risk (e.g., 3.5% or below) to drive improvements relative to the current state of risk in the field. This presents an additional challenge, however, in the precision of current IRFs in the low-risk range – due to the limited test data sample size available to fit traditional IRFs, the current IRFs likely exhibit limited precision when discerning the very fine gradations of risk at low risk levels. This may be at least partially addressed by adjusting the age range that we are targeting for risk prediction to older ages, who tend to exhibit greater risk for a given exposure (and for whom we have greater amounts of injury tolerance data from reference tests with post mortem human surrogates). Ultimately, however, increasing the precision of IRFs may require revisiting our approach to IRF development, potentially leveraging advanced means to augment the limited test data with simulations or with field data to increase the amount of information available to develop the IRFs (potentially combining data sources with advanced statistical techniques such as Bayesian analyses).

Further, evaluation in high-exposure, lower-speed collisions requires an occupant modelling tool that will be sensitive to changes in restraint design in a biofidelic manner in the target speed range. This sensitivity to restraint system changes can be affected by factors such as the body region coupling, dictated by the stiffness of the interconnecting components (e.g., the spine). For example, it is possible that an occupant model with an artificially stiff spine may appear reasonably biofidelic in high-severity loading, yet may over-state the coupling stiffness between the body regions when exercised in lower-severity impacts. This may in turn obscure the true effects of changes to the restraints - for example, misstating the effects of load sharing between the lap belt, shoulder belt, and airbag. Thus, any effort to develop an evaluation method in low-to-moderate speed collisions should include a critical evaluation of the target occupant model (be it an ATD or human body model) to ensure that it will interact with the restraint systems in a biofidelic manner in that ΔV range.

CONCLUSIONS

Improving occupant restraint during high-severity frontal crashes may require injury criteria targets tailored for high severity collisions (striking a balance between feasibility and targets that are challenging enough to prompt an improvement relative to the current state of risk). In this study, we examined field data for belted occupants in frontal impacts to observe how injury patterns, severities, and risks change with collision severity. With these data we also examined the relative rates of injury across various body regions to provide a comparison for the relative rates of risk predicted in occupant simulations. In collisions with a ΔV at or above 60 km/h, the most common injuries were injuries to the ankle, tibia & fibula, femur, ribs, thoracic organs, brain, and lumbar spine, all of which occurred at relatively similar rates. This suggests that the injury risk for these injury types is relatively balanced in the field, with no individual injury type exhibiting a risk that was substantially greater than the others. This balance of injury risk was also observed in exemplar simulations of high severity crashes for all injury types except for hip injury (which tended to exhibit a much higher risk than the other injury types when predicted using the acetabulum injury risk function that has been proposed for the THOR-50M). The exemplar simulations and field data may also be used to identify a potential injury risk threshold that may serve as a target for high severity crash evaluations – for example, the simulations suggest that a target injury risk threshold of 40% may be feasible to achieve in the crash conditions studied using an improved restraint system, and would represent a substantial reduction in risk relative to that predicted with a contemporary restraint system. A target risk threshold of 40% would also likely represent an improvement relative to the contemporary risks observed in the field data for high severity crashes. Considering this, potential injury criteria values are presented targeting a risk threshold of 40% for each individual body region. Future work may include developing similar injury criteria targets tailored for use in low-speed crash evaluations (where collision exposure is very high), and translating to combined-probability criteria aggregating risk across body regions.

ACKNOWLEDGEMENTS

This study was supported by Autoliv Research. The opinions expressed here are solely those of the authors.

REFERENCES

[1] European Commission. 2020. European Road Safety Observatory Facts and Figures Buses / coaches / heavy goods vehicles - 2020. Brussels, European Commission, Directorate General for Transport. https://road-safety.transport.ec.europa.eu/system/files/2021-07/facts_figures_buses_and_hgv_final_20210323.pdf. Accessed 24.10.2022.

[2] Schindler R, Jänsch M, Bálint A, Johannsen H. 2022. Exploring European Heavy Goods Vehicle Crashes Using a Three-Level Analysis of Crash Data. Int J Environ Res Public Health. 2022 Jan 7;19(2):663. doi: 10.3390/ijerph19020663. PMID: 35055484; PMCID: PMC8775486.

[3] European Commission, Mobility and Transport. 2021. Road traffic Fatalities in the EU in 2019. https://road-safety.transport.ec.europa.eu/system/files/2021-11/DG%20MOVE%20ROAD%20SAFETY_INFOGRAPHICS_twitter.pdf. Accessed 24.10.2022.

[4] National Center for Statistics and Analysis. 2022. Traffic safety facts 2020: A compilation of motor vehicle crash data (Report No. DOT HS 813 375). National Highway Traffic Safety Administration.

[5] Adalian C, Russo JL, Cesari D and Desfontaines H. 1998. October. Improvement of car-to-truck compatibility in head-on collisions. In the Proceedings of the 16th International Technical Conference on the Enhanced safety of Vehicles (pp. 883-891).

[6] Goudswaard AP, Nieboer JJ. and Janssen EG. 1991. Truck front underrun protection. TNO Road-Vehicles Research Institute, Netherlands. IRCOBI.

[7] Krusper A, and Thomson R. 2008. Crash compatibility between heavy goods vehicles and passenger cars: structural interaction analysis and in-depth accident analysis. In International Conference on Heavy Vehicles.

[8] Thomson R, Edwards M, Martin T, Van der Zweep C, Damm R and Valle GD. 2007. Car-car crash compatibility: development of crash test procedures in the VC-Compat project. International journal of crashworthiness, 12(2), pp.137-151.

[9] Gabler HC and Hollowell WT. 2000. The crash compatibility of cars and light trucks. Journal of Crush Prevention and Injury Control, 2(1), pp.19-31.

[10] Mroz K, Östling M, Lubbe N. 2023. Passenger cars in head-on crashes with heavy goods vehicles: for what severity should future car restraint systems be designed? The 27th International Technical Conference on the Enhanced Safety of Vehicles Conference (ESV), Yokohama, Japan 2023. Paper Number 23-0060.

[11] Ostling M, Eriksson L, Dahlgren M, Forman J. 2022. Frontal head-on car-to-heavy goods vehicle crashes and their effect on the restraint system. The 27th International Technical Conference on the Enhanced Safety of Vehicles Conference (ESV), Yokohama, Japan 2023. Paper Number 23-0198.

[12] de Coo PJA, Blaauw GJ and Huijbers JJW. 1997. EEVC Working Group 14 Activities in Energy-Absorbing Front Underrun Protection. SAE heavy vehicle underride protection TOPTEC, 15-16 April, 1997, Palm Springs, CA, USA.

[13] Craig M, Parent D, Lee E, Rudd R, Takhounts E, Hasija V. 2020. Injury criteria for the THOR 50th male ATD. National Highway Traffic Safety Administration.

[14] Gepner B, Bollapragada V, Acosta SM, Park G and Forman J. 2017. Comparison of THOR LX Xversion and Dorsiflexion Response in Component Tests, Sled Tests and Full Vehicle Crash Tests. In 25th International Technical Conference on the Enhanced Safety of Vehicles (ESV) National Highway Traffic Safety Administration.